Box 2.17 Bouguer anomaly

The Bouguer anomaly (Δg_B) is the difference between the observed value (g_{obs}), duly corrected, and a value at a given base station (g_{base}), such that:

$$\Delta g_B = g_{obs} + \Sigma(\text{corr}) - g_{base}$$

with

$$\Sigma(\text{corr}) = \delta g_L + (\delta g_F - \delta g_B) + \delta g_{TC} \pm \delta g_{EC} \pm \delta g_{IC} - \delta g_D$$

where the suffices refer to the following corrections:

L = latitude; F = free-air; B = Bouguer;
TC = terrain correction; EC = Eötvös correction;
IC = isostatic correction; and D = drift (including Earth tides).

2.6 INTERPRETATION METHODS

There are two approaches to the interpretation of Bouguer anomaly data. One is *direct* where the original data are analysed to produce an interpretation. The other is *indirect*, where models are constructed to

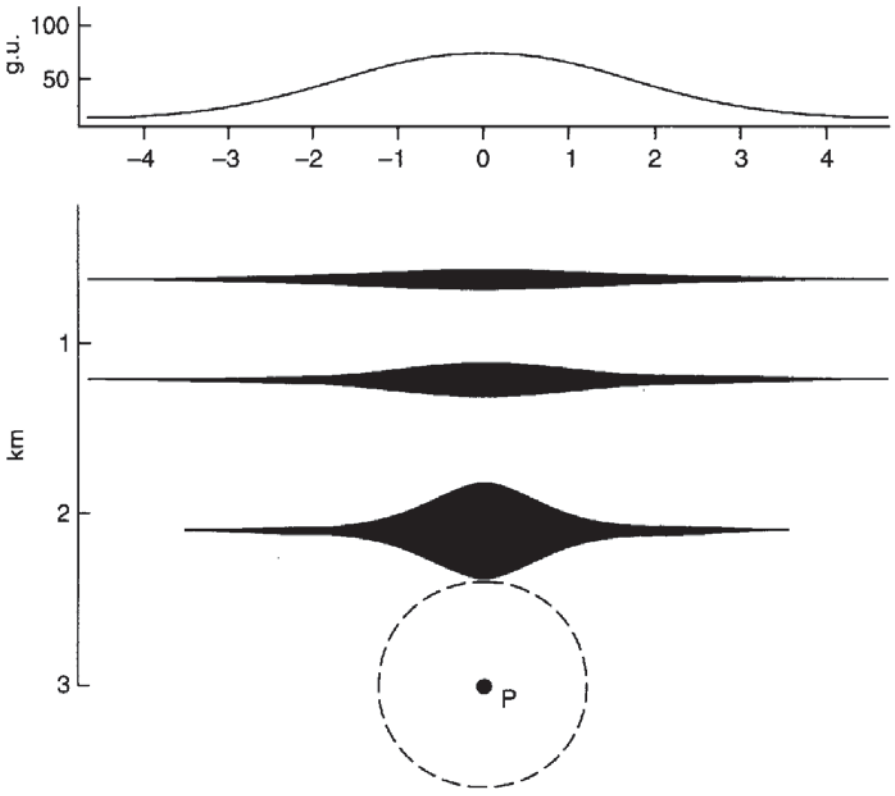

Figure 2.24 Ambiguity in geological models, all of which produce the gravity anomaly shown at the top. The lens-shaped bodies have a gravity anomaly identical to that of a sphere at P of radius 600 m and density contrast 1.0 Mg/m^3. The thickness of the bodies is exaggerated by a factor of 3. From Griffiths and King (1981), by permission

compute synthetic gravity anomalies which are compared in turn with the observed Bouguer anomaly. The model producing the best fit, however, will not be unique as several alternative models may be found which also produce an equivalent fit (Figure 2.24). It is because of this type of ambiguity, which has already been discussed in Section 1.2 (see also Figure 1.1), that different geophysical methods are used together to constrain the geologic model.

2.6.1 Regionals and residuals

Bouguer anomaly maps are rather like topographic maps with highs and lows, linear features and areas where the contours (*isogals*) are closely packed and others where they are further apart. There may be a gentle trend in the gravity data, reflecting a long-wavelength gravity anomaly attributable to deep-seated crustal features; this is known as a *regional anomaly*. Shorter-wavelength anomalies arising from shallower geological features are superimposed on the regional anomaly, and it is these anomalies that are often to be isolated for further analysis. Separation of the regional from the Bouguer anomaly will leave a *residual anomaly* (Figure 2.25).

There are a number of different methods with varying degrees of complexity and effectiveness by which residual anomalies can be isolated (Nettleton, 1954). These range from curve-sketching, which is purely subjective, through to computer-based analytical methods. Graphical methods include sketching in estimated regional trends by eye on a profile (Figure 2.25A) or calculating the residual from estimated isogals on a map. Figure 2.25B illustrates how the residual is calculated. The 5.0 mGal isogal, which has been highlighted, intersects several estimated regional isogals. At points A and B, the difference (i.e. the residual) between the 5.0 mGal line and those it crosses are respectively +0.2 and +0.4 mGal and contours are drawn of the same residual value.

An example of the quantitative analytical method consists in fitting a low-order polynomial expression to the Bouguer anomaly data and then subtracting the calculated values from those observed to produce residual values, which are then plotted in map form. A more sophisticated method is the application of Fourier analysis by which a power spectrum is obtained for the Bouguer anomaly (Spector and Grant 1970; Syberg 1972). This highlights the different wavelengths of anomaly present and so allows a form of filtering to be undertaken to remove the unwanted anomalies (e.g. Granser *et al.* 1989). Dobrin (1976), Grant and West (1965) and Telford *et al.* (1990) discuss the various techniques in more detail.

Although the analytical methods appear more rigorous and thorough, there are occasions when the manual interpretation can take into account known variations in local geology more readily than an automated system.

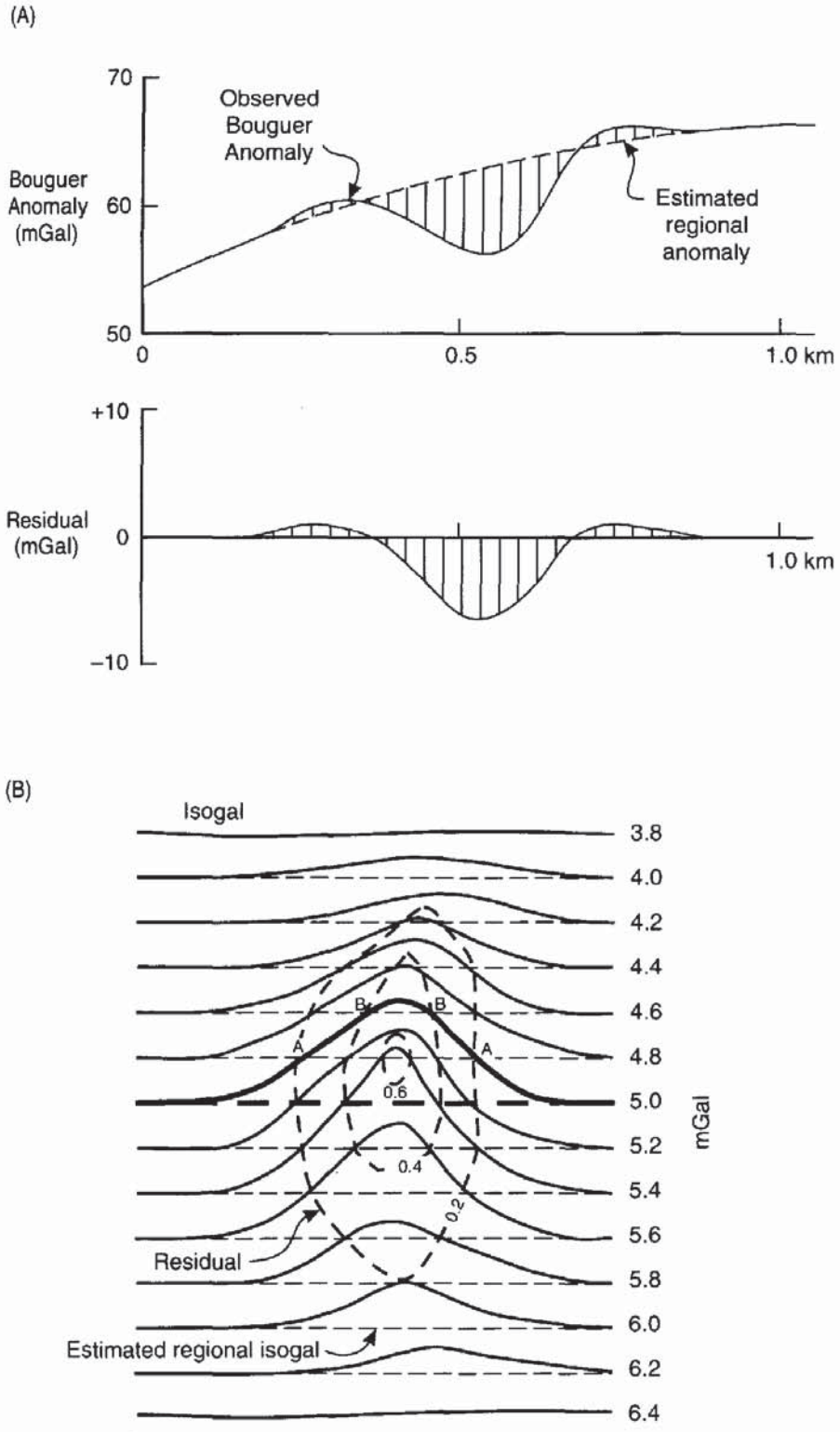

Figure 2.25 (A) Removal of a residual gravity anomaly from a regional profile, and (B) how a residual gravity map is constructed (see text for an explanation). After Dobrin (1976), by permission

2.6.2 Anomalies due to different geometric forms

Certain geologic structures can be approximated to models with known geometric forms (Nettleton, 1942). For example, a buried cavity may be represented by a sphere, a salt dome by a vertical cylinder, a basic igneous dyke by an inclined sheet or prism, etc. Another factor to be considered is whether the target to be modelled should be considered in two or three dimensions. If g is computed across a profile over a buried sphere, then that profile should hold true for any direction across the sphere. However, if the profile is across a buried horizontal cylinder, then the profile along the long-axis of the cylinder will be quite different from that across it. Also, if the strike length of the feature is greater than 20 times any other dimension, then it may be considered a two-dimensional body. Where this does not hold true, any profile will also sense the effects of the third dimension ('edge effects') and thus will not be modelled accurately if considered only in two dimensions.

Several common geometrical forms are illustrated in Figure 2.26, with their associated gravity profiles and the types of geologic features they approximate. The equations used to calculate the maximum anomaly for each geometric feature are given in Box 2.18. No attempt is made here to explain the derivations of these formulae, all of which are discussed much more fully by Dobrin (1976), Telford *et al.* (1990) and Parasnis (1986). The equations in Box 2.18 are intended only as guides to estimate the maximum values of the associated gravity anomalies. The use of the half-width ($x_{1/2}$) is discussed in more detail in Section 2.6.3 and 2.6.4.

The range of geometric forms given above is by no means complete. Details of other forms and their interpretations, such as by the use of characteristic curves, are given by Grant and West (1965) and Telford *et al.* (1990).

Calculation of gravity anomalies using the above methods should be regarded as a first step in the interpretation process. There are other, more sophisticated, and commonly computerised methods of gravity anomaly analysis. However, it is worth noting that for more complicated geological features of irregular shape which do not approximate to any of the geometrical forms, two other broad approaches can be adopted. The first is the use of graphical methods, and the second is an analytical approach. In the graphical methods, a template, which is divided into segments, is superimposed on an irregular cross-section of the geological feature to be modelled. The gravity at a point on the surface can be calculated by summing the effects of all the individual segments covering the cross-section of the feature.

Graphical methods can also be used for three-dimensional bodies. In this case, the appropriate template is superimposed on contours of the geological feature in the horizontal plane, thereby dividing it into

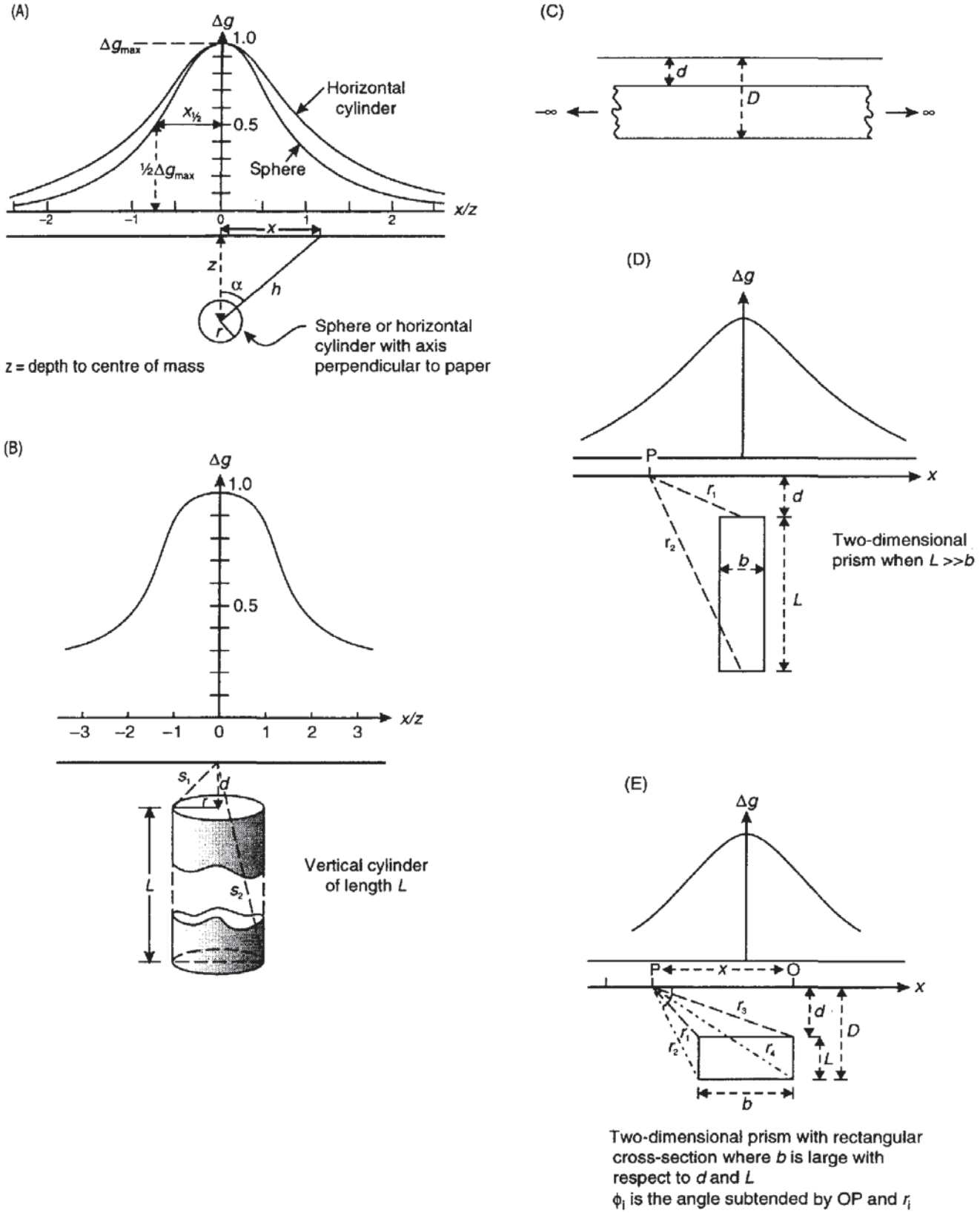

Figure 2.26 Representative gravity anomalies over given geometric forms: (A) a sphere or horizontal cylinder with its long axis perpendicular to the paper; (B) a vertical cylinder; (C) a semi-infinite horizontal slab (a Bouguer plate when $d = 0$); (D) a vertical rectangular prism; and (E) a horizontal rectangular prism

Box 2.18 Gravity anomalies associated with geometric forms
(see Figure 2.26)

Models	Maximum gravity anomaly	Notes
Sphere	$\Delta g_{max} = (4/3)\pi G\delta\rho r^3/z^2$	$z = 1.305x_{1/2}$ (m)
Horizontal cylinder	$\Delta g_{max} = 2\pi G\delta\rho r^2/z$	$z = x_{1/2}$
Vertical cylinder	$\Delta g_{max} = 2\pi G\delta\rho\,(s_1 - d)$	If $L \rightarrow$ infinity
	$\Delta g_{max} = 2\pi G\delta\rho r$	If $d = 0$
	$\Delta g_{max} = 2\pi G\delta\rho\,(L + s_1 - s_2)$	If L finite
		$z = x_{1/2}\sqrt{3}$
Buried slab (Bouguer plate)	$\Delta g_{max} = 2\pi G\delta\rho L$	For $L = 1000$ m and $\delta\rho = 0.1$ Mg/m^3, $\Delta g_{max} = 42$ g.u.
Infinite slab	$\Delta g_{max} = 2\pi G\delta\rho\,(D - d)$	
Horizontal rectangular prism	$\Delta g_p = 2G\delta\rho\left[x\ln\left(\frac{r_1 r_4}{r_2 r_3}\right) + b\ln\left(\frac{r_2}{r_1}\right) + D(\phi_2 - \phi_4) - d(\phi_1 - \phi_3)\right]$	
Vertical rectangular prism	$\Delta g_{max} = 2G\delta\rho[b\ln(d/L)]$	$L \gg b$
Step	$\Delta g_{max} = 2G\delta\rho\,[x\ln(r_4/r_3) + \pi(D - d) - D\phi_4 + d\phi_3]$	

All distances are in metres unless stated otherwise; Δg_{max} in mGal and $\delta\rho$ in Mg/m^3, and the factor $2\pi G = 0.042$.

a pile of horizontal slabs each with a thickness equal to the contour interval.

Most computer-based analytical methods (e.g. Bott 1960) are based on the premise proposed by Talwani *et al.* (1959), that a cross-section of a two-dimensional body can be approximated by representing it by a multisided polygon (Figure 2.27A). This was developed by Talwani and Ewing (1960) for three-dimensional bodies (Figure 2.27B) which are approximated by a stack of polygonal laminae. The gravity effect of each lamina is computed and summed to give a total gravity anomaly. Enhancements of these methods have largely been centred on improving the ease of use of the software on computers that have dramatically increased in power and efficiency, and on the portability of software from mainframe machines to personal microcomputers (Busby 1987).

A development of the three-dimensional approach is to consider a geological body as a stack of cubic blocks of uniform size, each

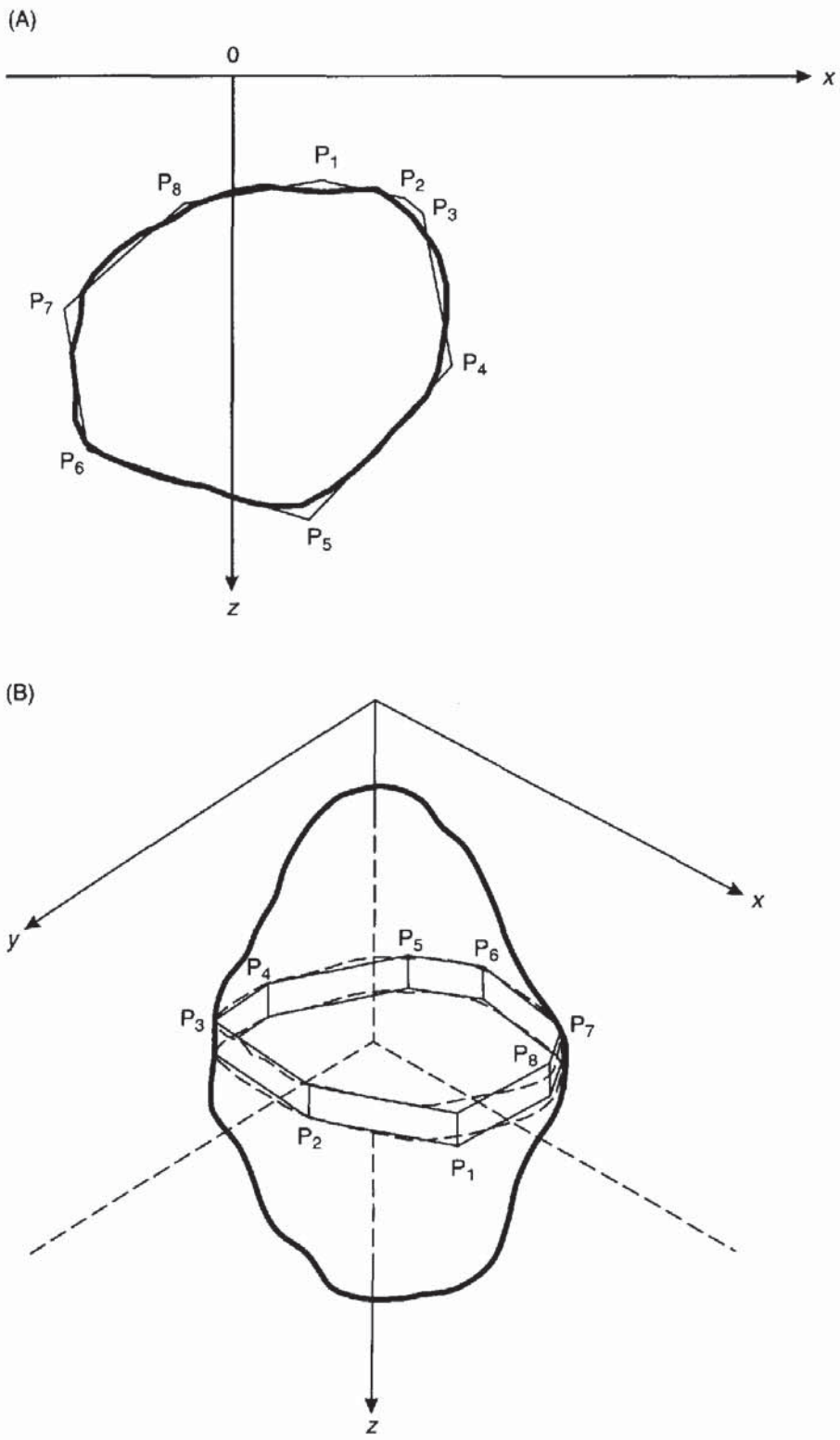

Figure 2.27 (A) Polygonal representation of an irregular vertical section of a two-dimensional geological feature. (B) Representation of an irregular three-dimensional geological feature by polygonal laminae

having a specified density contrast. Each little cube is considered as a point mass and thus the total gravity anomaly for the entire body is obtained by summing the constituent gravity components for each mini-cube. The resultant gravity anomaly is compared with that

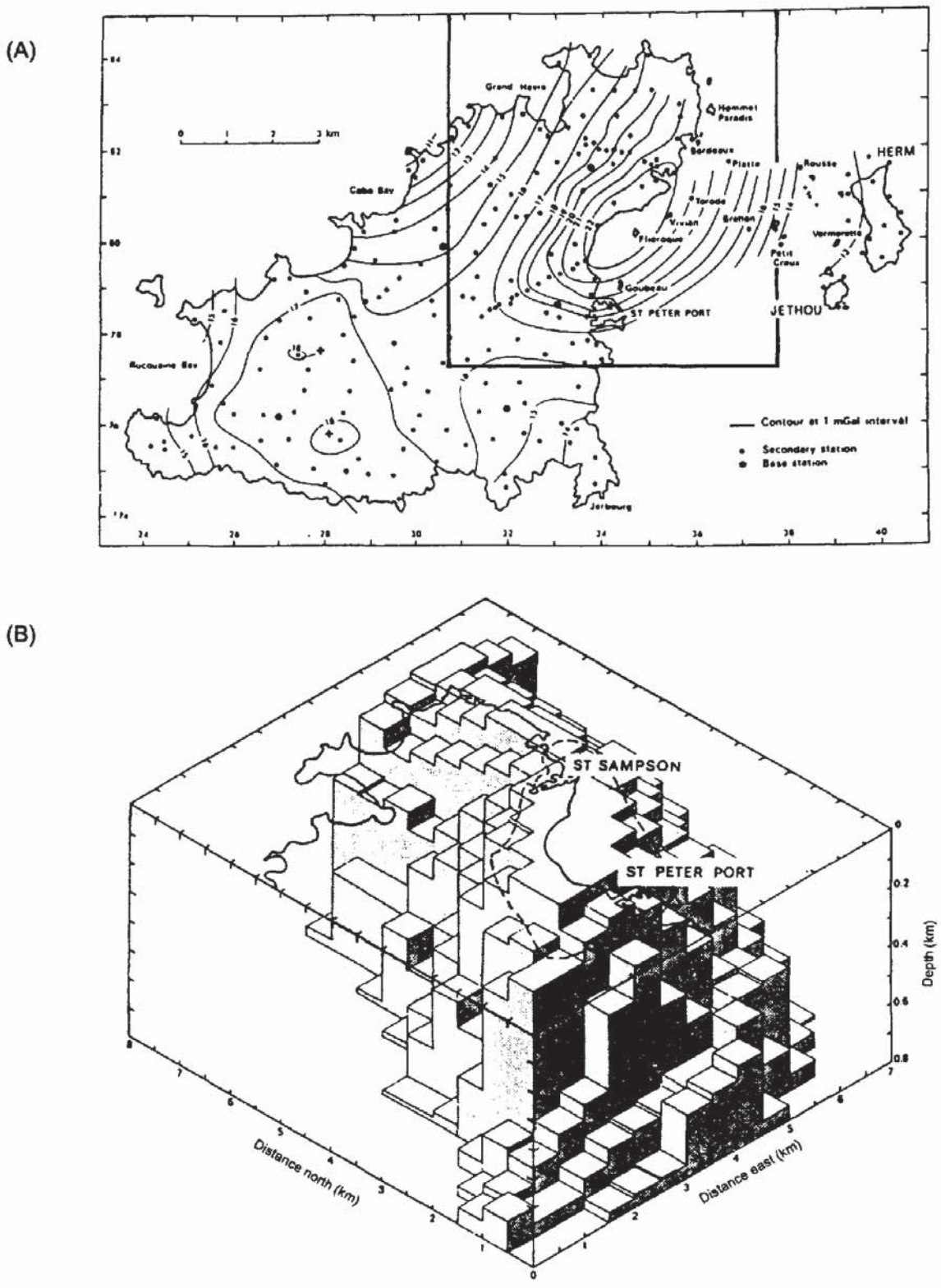

Figure 2.28 (A) Bouguer anomaly map for Guernsey, Herm and Jethou, Channel Islands, and (B) a three-dimensional model of the underlying St Peter Port Gabbro (density contrast 0.27 Mg/m^3, vertical exaggeration 5:1). The coastline and the outline of the gabbro outcrop are indicated. The gabbro is thus interpreted as a laccolith approximately 4 km in diameter and 0.8 km thick. From Briden *et al.* (1982), by permission

observed and, if necessary, the model is adjusted by trial-and-error or by automatic iterative methods (e.g. non-linear optimisation (Al-Chalabi 1972)) until the differences between the computed and observed anomalies are reduced to an acceptable, statistically defined level. Better resolution is obtained by reducing the size and increasing the number of individual cubes within the model. By having a regular cube size, the computation is eased considerably. An example of the application of this technique is given in Figure 2.28, where gravity data from Guernsey, Channel Islands, have revealed that a gabbro body, which outcrops to the north-east of the island near St Peter Port, has the form of a laccolith 0.8 km thick and about 4 km in diameter (Briden *et al.* 1982).

2.6.3 Depth determinations

Of major importance in the interpretation of any gravity data is the determination of depth to the centre of mass and/or to the top of the body causing the anomaly. The maximum depth at which the top of any particular geological body can be situated is known as the *limiting depth*. Methods of obtaining this information depend on which interpretational technique and model are being used. Let us consider various *direct* or *forward* methods where the actual gravity anomaly data are used to derive depths and also estimates of anomalous masses of the features causing the anomalies.

The commonest rules of thumb concern the use of the half-width of the anomaly; that is, the half-width ($x_{1/2}$) of the anomaly where the amplitude is half the maximum value (see Figure 2.26). Some workers define the half-width as the entire width of the anomaly at half peak amplitude and the form of the depth and mass determination equations will differ accordingly. Whichever formulae are used, care should be taken when calculating the limiting depth. The causative body has finite size and its mass is not concentrated at its centre of mass, and thus any estimate of depth will be overestimated. Also, the method will only give an approximation of depth in cases where all the constituent components have the same sense of density contrast (i.e. all negative or all positive). These formulae will also not be effective for compact mineral bodies. Formulae for a selection of given geometric forms are given in Box 2.19A and an example of one calculation is given in Box 2.19B.

Several basic 'rules', known as the *Smith Rules* after their originator (Smith 1959, 1960), have become established in the calculation of limiting depths. Two rules (1 and 2 in Box 2.20) use a *gradient–amplitude ratio* method. Consider any geological body that gives an isolated gravity anomaly (Figure 2.30) entirely of either sign with a maximum gravity (Δg_{max}) that varies along the line of the profile and thus has a horizontal gradient which reaches a maximum value at $\Delta g'_{max}$. The Smith Rules describe the various relationships between

the limiting depth d to the top of any geological body and the maximum gravity (Δg_{max}) and its horizontal gradient ($\Delta g'_{max}$) as listed in Box 2.20.

Box 2.19A Depth estimates for given geometric forms

Form	Formula	Notes
Sphere	$z = 1.305x_{1/2}$	z is depth to centre of mass
	$d = z - r$	d is depth to top of sphere of radius r
		$r^3 = \lvert\Delta g_{max}\rvert z^2/(0.028\delta\rho)$ from Box 2.18
Horizontal cylinder	$z = x_{1/2}$	z is depth to cylinder axis
	$d = z - r$	d is depth to top of cylinder of radius r
		$r^2 = \lvert\Delta g_{max}\rvert z/(0.042\delta\rho)$ from Box 2.18
Vertical cylinder	$z = 1.732x_{1/2}$	z is depth to top end of cylinder (overestimates z)
Thin dipping sheet	$z \approx 0.7x_{1/2}$	z is depth to top of sheet
	$z \approx x_{1/2}$	When $z \approx$ dip length of sheet
		When $z \gg$ dip length of sheet
		When length of sheet is very large or sheet dips at less than 60°, *no solution is possible*
Thick prism	$z = 0.67x_{1/2}$	z is depth to prism top = prism width, and depth to prism base is twice width
	$z = 0.33x_{1/2}$	When depth to prism base is 10 times prism width
		In both cases, estimates of z are unreliable

Box 2.19B Example of calculation for a sphere

An air-filled cavity in rock of density 2.5 Mg/m^3 can be modelled by a sphere of radius r and depth to centre of mass, z (m). The resultant gravity anomaly is shown in Figure 2.29. Given $\Delta g_{max} = 0.048$ mGal, $x_{1/2} = 2.2$ m, and $\delta\rho = 2.5$ Mg/m^3:

$$z = 1.305 \times 2.2\,\text{m} = 2.87\,\text{m}.$$

Radius of sphere = r:

$$r^3 = 0.048 \times (2.87)^2/(0.0286 \times 2.5) = 5.53\,\text{m}^3.$$

continued